Compositional and Black Oil Reservoir Simulation

K.H. Coats, SPE, K.H. Coats and Co. Inc., and **L.K. Thomas,** SPE, and **R.G. Pierson,** SPE, Phillips Petroleum Co.

Summary

This paper describes a three-dimensional (3D), three-phase reservoir simulation model for black oil and compositional applications. Both implicit pressure, explicit saturation/concentration (IMPES) and fully implicit formulations are included. The relaxed volume balance concept effectively conserves mass and volume and reduces Newton iterations in both formulations. A new implicit well rate calculation method improves IMPES stability. It approximates wellbore crossflow effects with high efficiency and relative simplicity in both IMPES and fully implicit formulations. Multiphase flow in the tubing and near-well non-Darcy gas flow effects are treated implicitly.

Initial saturations are calculated as a function of water/oil and gas/oil capillary pressures, which are optionally dependent upon the Leverett J function. A normalization of the relative permeability and capillary pressure curves is used to calculate these terms as a function of rock type and gridblock residual saturations.

Example problems are presented, including several of the SPE comparative solution problems and field simulations.

Introduction

This paper describes a numerical model for simulating 3D, three-phase flow in heterogeneous, single-porosity reservoirs. The model incorporates black oil and fully compositional capabilities formulated in both IMPES and fully implicit modes. The formulations include a relaxed volume concept and a new method for implicit treatment of well rates with wellbore crossflow. The usual viscous, gravity, and capillary forces are represented by Darcy's law modified for relative permeability. The flow is isothermal although, as an option, a spatially variable, time-invariant temperature distribution may be specified in the compositional case.

Complex reservoir geometries, including pinchouts and non-neighbor connections across faults, can be simulated with Cartesian *xyz* or corner point geometry grids. Mapping or linear indexing is used to require storage and arithmetic only for active gridblocks.

The black oil option includes the r_s stb/scf term as well as the normal R_s solution gas term. It therefore applies to gas condensate and black oil problems. Interfacial tension, modifying gas/oil capillary pressure, is also entered vs. pressure in the black oil pressure/volume/temperature (PVT) table. The compositional case uses the Peng Robinson (PR)[1] or Soave Redlich Kwong (SRK)[2] equation of state (EOS). Shift factors[3] are included to account for volume translation.[4] The compositional case optionally uses tabular *K* values vs. *p*, rather than EOS fugacity-based *K* values. The table is generated internally by an expansion of the original reservoir fluid. This option applies near-rigorously to cases of natural depletion with or without water injection and/or influx. It is significantly more efficient than the use of the EOS in the IMPES case.

The effect of pore collapse and compaction is incorporated in the model applying the logic presented by Sulak *et al.*,[5] which has been expanded to include a water weakening effect.[6] Hysteresis of rock compressibility is included in the calculation to account for the irreversible effect of pore collapse. 3D compaction tables relate rock compressibility to porosity, water saturation, and stress. Each gridblock is then assigned to one of these tables. If no tables are entered, then porosity is $\phi_b\,[1 + c_r\,(p - p_b)]$, where ϕ_b is entered for each gridblock.

Copyright 1998 Society of Petroleum Engineers

This paper (SPE 50990) was revised for publication from paper SPE 29111, first presented at the 1995 SPE Symposium on Reservoir Simulation, 12–15 February. Original manuscript received for review 15 February 1995. Revised manuscript received 20 May 1998. Paper peer approved 3 June 1998.

IMPES and fully implicit formulations are coded for both the black oil and compositional cases. The linear solvers include direct D4,[7] nested factorization,[8,9] and red/black ILU/Orthomin.[10] Well rate terms including wellbore crossflow are implicit in both formulations. The wellbore constraint equations[11,12] are fully implicit to achieve exact target rates, even in the IMPES case.

Platform or gathering center logic allows assignment of target rates and constraints to groups of wells. Gas can be reinjected, taking into account available produced and outside gas, gas sales, and fuel loss. Produced gas from one platform can be transferred for injection on another platform.

The model handles the case of multiple reservoirs, e.g., stacked reservoirs, with no transmissibility communication between any pair of reservoirs and no well completed in more than one reservoir. This capability can reduce central processing unit (CPU) time by a factor of two or more, because the different reservoirs do not require the same number of Newton or linear solver iterations.

Tracer fractions for any number of traced components can be calculated. This feature is useful in equity situations as well as tracking injected gas streams. Traced components can be any of the fluid components including water. These calculations increase run times very little and are optional.

Following model description, several example problems are presented. They include five SPE Comparative Solution Project problems, a non-Darcy gas flow problem, a crossflow problem, and two field studies.

Mathematical Description of the Model

The model consists of $N = 2N_c + 4$ equations for each active gridblock and N_w well constraint equations for active wells that are not on pressure constraint. The N equations include mass balances for N_c hydrocarbon components and water.

$$\frac{V}{\Delta t}\bar{\delta}[\phi(\rho_o S_o x_i + \rho_g S_g y_i)]$$

$$= \Delta\left[T\rho_o x_i \frac{k_{ro}}{\mu_0}(\Delta p - \Delta P_{cgo} - \gamma_o \Delta Z)\right]$$

$$+ \Delta\left[T\rho_g y_i \frac{k_{rg}}{\mu_g}(\Delta p - \gamma_g \Delta Z)\right] - q_i,$$

$$i = 1, 2, \ldots, N_c \quad \ldots\ldots\ldots\ldots\ldots\ldots\ldots\ldots\ldots\ldots\ldots\ldots \text{(1a)}$$

$$\frac{V}{\Delta t}\bar{\delta}(\phi b_w S_w)$$

$$= \Delta\left[Tb_w \frac{k_{rw}}{\mu_w}(\Delta p - \Delta P_{cgo} - \Delta P_{cwo} - \gamma_w \Delta Z)\right] - q_w. \quad \ldots\ldots \text{(1b)}$$

In addition to these $N_c + 1$ equations, there are $N_c + 3$ constraint equations for each gridblock: N_c phase equilibrium constraints, and the summations to 1.0 of y_i, x_i, and S_w,S_o,S_g.

It is well known that a black oil PVT table including formation volume factors, R_s and r_s vs. pressure can be converted to compositional mode. The converted table gives the saturated oil and gas phase molar densities [moles/reservoir barrel (RB)] and compositions (mole fractions x_1 and y_1) as single-valued functions of pressure. Thus, Eqs. 1 and the constraints apply unchanged to the black oil case. Only the implicit and IMPES formulations require description with appropriate comment regarding compositional EOS PVT vs. the simpler black oil PVT.

The model formulation is an alteration of one previously described.[13] That paper's linearization renders the model equations

for a gridblock in the single matrix equation form,

$$C\delta P = \Delta(T\Delta\delta P) + R. \quad \ldots\ldots\ldots\ldots\ldots\ldots\ldots\ldots\ldots\ldots (2)$$

Transmissibility T and C are $N_c + 1$ x $N_c + 1$ matrices and unknown P, and residual R are $N_c + 1$ column vectors. The T matrix elements are calculated using upstream phase mobilities, densities, and compositions. In the IMPES, case T is empty except column $N_c + 1$. That column, T_{N_c+1}, contains the pressure transmissibilities, calculated using explicit phase mobilities, densities, and compositions.

The N variables selected in this linearization process are the natural ones $P = y_i, x_i, S_w, S_o, S_g, p$. This selection leads to simplicity in constraint expressions and no need for pivoting in Gaussian eliminations. Many authors propose a variety of other variable choices.[14,15,16]

Any term X in Eq. 1 has the general form of a product $X = abc$, and its value at time level $n + 1$ is approximated by the linearizations applying the latest iterate l information.

$$X_{n+1} \cong X^{l+1} = X^l + \delta X$$

$$\delta X = bc\ \delta a + ac\ \delta b + ab\ \delta c$$

$$\delta a = \sum_{m=1}^{N} \left[\frac{\partial a}{\partial \bar{P}_m} \delta \bar{P}_m \right] \quad \ldots\ldots\ldots\ldots\ldots\ldots\ldots\ldots\ldots\ldots (3)$$

For a three-phase block, the constraints are a set of $N_c + 3$ equations in the N variables. Gaussian elimination on them gives an elimination matrix E relating the $N_c + 3$ eliminated variables to the $N_c + 1$ retained or primary variables P of Eq. 2,

$$\delta P_e = E\ \delta P. \quad \ldots\ldots\ldots\ldots\ldots\ldots\ldots\ldots\ldots\ldots\ldots\ldots\ldots (4)$$

The $N_c + 3$ variables δP_e are eliminated from the linearized form of Eq. 1 by means of this matrix E. E is ostensibly an $N_c + 3$ x $N_c + 1$ matrix. Actually it is an N_cx$N_c + 1$ matrix because of the simplicity of the three constraints

$$\delta x_{N_c} = -\delta x_1 - \delta x_2 - \ldots - \delta x_{N_c-1} \quad \ldots\ldots\ldots\ldots\ldots\ldots (5a)$$

$$\delta y_{N_c} = -\delta y_1 - \delta y_2 - \ldots - \delta y_{N_c-1} \quad \ldots\ldots\ldots\ldots\ldots\ldots (5b)$$

$$\delta S_w = \alpha - \delta S_o - \delta S_g, \quad \ldots\ldots\ldots\ldots\ldots\ldots\ldots\ldots\ldots (5c)$$

where α is discussed below. The N_c eliminated variables in P_e are $y_1, y_2, \ldots, y_{N_c-1}, x_1$. E is formed at the beginning of each Newton iteration for each three-phase block and stored. The eliminated variables are then calculated from Eqs. 4 and 5 after P is available from the linear solver's solution of Eq. 2.

For a three-phase block, the resulting set of $N_c + 1$ primary variables is $x_2, x_3, \ldots, x_{N_c-1}, S_o, S_g, p$. The primary variables are $x_1, x_2, \ldots, x_{N_c-1}, S_o, p$ for a water/oil block and $y_1, y_2, \ldots, y_{N_c-1}, S_g, p$ for a gas/water block.

The units of each term in Eq. 2 are moles/d (STB/D for the last, water equation). For an all-water block, C is a diagonal matrix. For $i = 1, N_c$, $c_{ii} = 1/\Delta t$, $c_{N_c+1,N_c+1} = \partial\phi b_w/\partial\rho\ V/\Delta t$. If hydrocarbons invade the block, then the values of P_i, $i = 1,N_c$ are directly the number of moles of component i in the block. Thus, the mass, composition, density, and saturation of the hydrocarbon phase(s) can be computed, and the block is switched to the appropriate hydrocarbon/water case.

A significant difference from the above formulation is a relaxed volume concept mentioned by several authors in connection with IMPES. IMPES is an implicit pressure, explicit saturation method independently conceived by Stone and Garder[17] and Sheldon *et al.*[18] Their method is widely used in black oil simulation, generally incorporating the saturation constraint $S_w + S_o + S_g = 1$. However, early papers by Wattenbarger[19,20] and Abel *et al.*[21] described IMPES in the compositional and black oil cases with exact mass balance and a relaxed volume balance. Young and Stephenson[14] and others[15,16] more explicitly described the exact mass balances attained by relaxing the volume balance.

We use this concept in both the IMPES and implicit formulations. The saturation constraint is written as Eq. 5c where α is $1 - (S_w + S_o + S_g)$.[1] For both IMPES and implicit cases, the calculation procedure begins as follows. E and the coefficients for all terms C, T, and R of Eq. 2 are calculated at iteration l. In the implicit case, Eq. 2 and the well constraints are then solved by the linear solver. The solution vector P is (only) used to calculate well rate and interblock flow terms at the $l + 1$ iterate level. The mass of each component in the gridblock at iterate $l + 1$ is then calculated as the mass at time level n plus the net interblock inflow minus the production. The composition and density of each phase are then calculated, with only the pressure component of the solution vector P. S_w is calculated as the mass of water present divided by $l + 1$ level water density and pore volume (PV). For a three-phase block, the total hydrocarbon moles are flashed to obtain moles of gas and oil and the phase densities. The oil and gas volumes are calculated as their mass/density and saturations as volumes divided by $l + 1$ level PV. Thus, the three saturations do not add to unity, and α is not zero; but mass balance is exact for all components.

In effect, this procedure amounts to iterating out volume balance rather than mass balance. This introduces another (volume) balance to monitor and report with attendant closure tolerance considerations. In all problems to date, we have found this concept an improvement with results showing near-exact volume balance in addition to exact mass balance. Iterations and CPU time are somewhat significantly less, and the answers are the same as compared with the conventional 1.0 volume balance approach.

In the IMPES case, the pressure transmissibilities T_{N_c+1} are not necessarily constant over the timestep. If more than one Newton iteration is performed, they are recalculated to account for possible changes in flow direction. The IMPES pressure equation is obtained in a straightforward manner,[22] applying the obvious extension of the original black oil IMPES reduction. The ith equation of the $N_c + 1$ scalar equations comprising Eq. 2 is multiplied by a factor v_i, with $v_{N_c+1} = 1$, and the resulting $N_c + 1$ equations (rows) are added. The values of v_i are determined so that this addition reduces the left-hand side to a single term $c\delta p$. Let A be the N_cxN_c matrix obtained by deleting row $N_c + 1$ and column $N_c \pm 1$ from C. Let the N_c-row vector B be the first N_c entries of the last row of C. Then the IMPES reduction vector v (first N_c entries) is obtained from their transposes as

$$A'v = -B'. \quad \ldots\ldots\ldots\ldots\ldots\ldots\ldots\ldots\ldots\ldots\ldots\ldots\ldots (6)$$

The reduction process gives three scalar transmissibilities τ that are simply the dot or scalar products $v \cdot T_{N_c+1}$. A fourth dot product $v \cdot R$ gives the scalar residual r and the IMPES pressure equation

$$c\delta p = \Delta(\tau\Delta\delta p) + r. \quad \ldots\ldots\ldots\ldots\ldots\ldots\ldots\ldots\ldots\ldots (7)$$

Because $v_{N_c+1} = 1$, the dot products require only N_c multiplies. This reduction process gives a left-hand pressure coefficient c, which reflects effects of changes in phase saturations, densities, and compositions.

Additional IMPES reduction is required to eliminate the nonpressure coefficients in the implicit bottomhole pressure constraints. The latter constraint includes an $N_c + 1$ row vector term for each perforated block. The first N_c (nonpressure) elements of this term are eliminated employing as pivots the diagonal elements of the C matrix of Eq. 2. This results in a constraint equation containing only pressure coefficient terms. However, the number of such terms is significantly larger than the number of perforated blocks.

For the compositional case, the N_c phase equilibrium constraints are equality of liquid and vapor fugacities for each component. For the black oil case, the E matrix has only one nonzero column.

$$\delta y_1 = \frac{dY_1(p)}{dp}\,\delta p \quad \ldots\ldots\ldots\ldots\ldots\ldots\ldots\ldots\ldots\ldots\ldots\ldots (8)$$

$$\delta x_1 = \frac{dX_1(p)}{dp}\,\delta p, \quad \ldots\ldots\ldots\ldots\ldots\ldots\ldots\ldots\ldots\ldots\ldots\ldots (9)$$

where the derivatives are obtained directly from the converted table.

In the compositional case, a Newton-Raphson flash calculation[23] is performed each Newton iteration for each three-phase block. It solves for $N_c - 1$ mole fractions and L or V. Phase disappearance is signaled by flash iterations outside the range $0 < L < 1$. For water/oil and gas/water blocks, Newton-Raphson p_{sat} calculations are performed, and phase appearance is signaled by the sign of $p - p_{sat}$. In the event of flash failure, the model calculates p_{sat} to confirm the hydrocarbon single-phase state. In the event of p_{sat} failure, the mixture is flashed at a lower pressure, and the resulting two phases are iteratively flashed back up toward block pressure p. The flash and/or p_{sat} calculations may fail either because of proximity to critical point or passing out the right-side of the pressure/composition phase envelope. The model avoids excessive flash, p_{sat} iterations, and calculations by applying stored historical data and avoiding repeated attempts when composition has not changed sufficiently. The model senses when composition has moved to the right of the phase envelope and avoids the futile flash and p_{sat} calculations there. Typically, a flash calculation requires only one to three Newton-Raphson iterations. Viscosities are obtained from the Lohrenz *et al.* correlation.[24] Interfacial tension is obtained from the McLeod-Sugden correlation.[25]

In the black oil case, a simple check of overall mole fraction z_1 against the converted table $X_1(p)$ value detects phase appearance or disappearance. In both black oil and compositional cases, a block's phase configuration may change over the Newton iterations.

Description of Well Calculations

Well calculations include the splitting or allocation of total well rate among the completed layers, the well constraint equation preserving target rate over the iteration, and special effects such as non-Darcy flow.

Holmes[26] described a splitting method that accounts for wellbore crossflow in implicit formulations. He assumed a fully mixed wellbore and used three wellbore variables, two phase volume variables, in addition to wellbore pressure. Modine *et al.*[27] described an implicit splitting method that uses multinode wellbore mass balances to eliminate the fully mixed assumption in crossflow.

The splitting method used here is one developed by Phillips Petroleum in the 1970's. It represents crossflow assuming a fully mixed wellbore and uses the single wellbore pressure variable. It is simple and more efficient than the method of Modine *et al.* Wellbore pressure is

$$p_w(Z) = p_w + \gamma_{wb}(Z - Z^*), \quad \ldots\ldots\ldots\ldots\ldots\ldots\ldots\ldots (10)$$

where wellbore gradient γ_{wb} is approximated at the beginning of the timestep and held fixed over the Newton iterations. We consider a production well completed in multiple layers of index k. Defining P_k as $p_k - \gamma_{wb}(Z_k - Z^*)$, the total RB/D Q_k and molar q_{ik} rates (moles/D) are the following:

For inflow layers ($P_k > p_w$)

$$Q_k = J_k\,\lambda_{tk}(P_k - p_w) \quad \ldots\ldots\ldots\ldots\ldots\ldots\ldots\ldots (11)$$

$$q_{ik} = J_k(\lambda_o\rho_o x_i + \lambda_g\rho_g y_i)_k(P_k - p_w) \quad \ldots\ldots\ldots\ldots\ldots\ldots (12)$$

$$q_{wk} = J_k\lambda_{wk}b_{wk}(P_k - p_w); \quad \ldots\ldots\ldots\ldots\ldots\ldots\ldots\ldots (13)$$

for outflow layers ($P_k < p_w$), Q_k is the same as Eq. 11 and

$$q_{ik} = J_k f_i\lambda_{tk}(P_k - p_w) \quad \ldots\ldots\ldots\ldots\ldots\ldots\ldots\ldots (14)$$

$$q_{wk} = J_k f_w\lambda_{tk}(P_k - p_w), \quad \ldots\ldots\ldots\ldots\ldots\ldots\ldots\ldots (15)$$

where $f_i = q_{i+}/Q_+$, $f_w = q_{w+}/Q_+$, and the + denotes summation over all inflow layers. That is, q_{i+} is the summation of all inflow-layer q_{ik} molar rates, Q_+ is the summation of all inflow-layer Q_k RB/D rates. This definition and use of f_i, f_w represents the fully mixed wellbore assumption; the outflow stream is the same for all outflow layers and has the composition of the combined inflow streams. The interphase mass transfer and compressibility effects within the wellbore are neglected. All terms in the above equations are known or calculable from the single unknown p_w.

The well target rate q^* may be specified in any of nine different units, including STB/D oil, Mcf/D gas, and total RB/D. For the simplest case of conventional black oil ($r_s = 0$, oil = component 1) and q^* = STB/D oil,

$$q^* = q_1 = q_{1+} + q_{1-} = q_{1+}\left(\frac{Q_-}{Q_+}\right), \quad \ldots\ldots\ldots\ldots\ldots\ldots (16)$$

where q_{1-} and Q_- are the summations of q_{1k} and Q_k over all outflow layers. All terms on the right side of Eq. 16 are single-valued functions of p_w. Eq. 16 is solved for p_w applying Newton-Raphson iteration and q_{ik}^l are calculated from Eqs. 12 and 14. The implicit molar rates required in the model are then

$$q_{ik} = q_{ik}^l + \delta q_{ik} = q_{ik}^l + \sum_{m=1}^{N}\frac{\partial q_{ik}}{\partial \bar{P}_m}\,\delta\,\bar{P}_m. \quad \ldots\ldots\ldots\ldots\ldots\ldots (17)$$

The f_i, f_w values are iteratively lagged. All other terms in the q_{ik} expressions are differentiated with respect to p_w and all reservoir gridblock variables y_i, x_i, S_w, S_o, S_g, and p.

The outflow curve gives p_w as either $p_w = BHP$ or as a function of q_o, gas/oil ratio, and water cut given by a tubinghead pressure table. If the calculated p_w from Eq. 16 is above the outflow curve, the well is on target rate, and a well constraint equation applies. If not, Eq. 16 and the outflow curve must be solved simultaneously for a p_w, which is an intersection of the inflow (Eq. 16) and outflow curves. In this case, there is no constraint equation if outflow $p_w = BHP$ but there is in the tubinghead pressure table case.[28]

The constraint equation for the above black oil example is

$$\sum_{k=k_1}^{k_2}\delta q_{lk} = 0. \quad \ldots\ldots\ldots\ldots\ldots\ldots\ldots\ldots\ldots\ldots (18)$$

In black oil cases, the constraint equation exactly preserves target rate. The compositional case is more difficult. With q^* = STB/D oil specified, the constraint equation holding constant total moles/D,

$$\sum_{k=k_1}^{k_2}\delta q_k = 0, \quad \ldots\ldots\ldots\ldots\ldots\ldots\ldots\ldots\ldots\ldots (19)$$

preserves surface oil rate only if the bottomhole inflow is an oil or gas phase of unchanging composition. The model uses a method[29] applying surface separation system overall K values. It gives a modified form of Eq. 18, which significantly reduces departure of the new rate from target value. This contributes to fewer Newton iterations, or better rates for the same number of iterations, in the compositional case.

It is well known that high velocity gas flow can affect gas injectivity in injection wells and producing rates and gas/oil ratio in production wells. Katz and Cornell[30] modified the Darcy flow equation to account for this effect by introducing the β factor in the Forscheimer equation. The model uses a radially integrated form of that equation to relate p_w and gas rate.[28]

$$p_k - p_{wk} = \left[\frac{1}{\lambda_g J\rho_g}\,q_g + \frac{41.125(10^{-16})M\beta}{\rho_g r_w h^2}\,q_g^2\right]_k. \quad \ldots\ldots\ldots (20)$$

The term h^2 is missing in Ref. 28, which describes in detail the modifications for non-Darcy flow in the layer gas rate calculation.

The β factor is presented graphically as a function of permeability and porosity by Katz *et al.*[31] The correlation of Firoozabadi[32] is used here,

$$\beta = f\frac{2.6(10^{10})}{(k_{rg}k)^{1.2}}, \quad \ldots\ldots\ldots\ldots\ldots\ldots\ldots\ldots (21)$$

where f may be entered as data for each perforated layer.

The effect of non-Darcy flow can also be expressed in terms of an apparent skin that varies with flow rate and is added to the laminar skin value.

$$s_{total} = s + Dq_g. \quad \ldots\ldots\ldots\ldots\ldots\ldots\ldots\ldots\ldots\ldots (22)$$

The equation for calculating the non-Darcy flow coefficient, D, is comprised of the effects of three components for a perforated well: the compacted zone around perforation tunnels, the damaged zone because of drilling fluids, and the reservoir rock properties.[33,34] These near wellbore effects can result in an equivalent β factor for poorly stimulated wells that is several orders of magnitude larger than values calculated for reservoir rock.

$$\beta_{effective} = \frac{hr_w\mu_g D}{2.226(10^{-15})k_{rg}rG} \quad \ldots\ldots\ldots\ldots\ldots\ldots\ldots\ldots\ldots\ldots (23)$$

Values of f in Eq. 21 can be calculated as the ratio of $\beta_{\text{effective}}$ divided by the β for reservoir rock.

Well Calculation Examples

Two examples are presented to illustrate the well calculation features in the model. First, an example that contains a considerable amount of wellbore crossflow is presented. Next, an example that includes the additional pressure drop, which results from non-Darcy flow in the near wellbore region, is discussed. All simulations reported in this paper were run on an IBM RS6000/590 using the XLF 3.1 compiler.

Wellbore Crossflow Example

We have noted good accuracy of the wellbore crossflow method presented here in a number of x-z cross-sectional problems. 3D dual-slice versions of such cross sections can be run to give exact results.[28] The test problem presented here is a variant of the SPE2 10 x 15 r-z coning problem. The grid is a 10 x 15 x-z cross section 2,500 ft wide and 2,000 ft long with Δx equal to 200 ft. Data unchanged from SPE2 include layer properties, black oil PVT data, and relative permeability/capillary pressure data.

Depth to top center of gridblock (1,1,1) is fixed at 9,000 ft, and the grid is rotated by a dip angle of 5.7°, depths increasing with increasing x. Zero vertical permeability is assigned between Layers 5 and 6 and between Layers 10 and 11, resulting in three isolated layer groups.

Initial conditions are capillary/gravitational equilibrium with a pressure of 3,600 psia at a gas/oil contact depth equal to 9,070 ft and with a water/oil contact depth of 9,370 ft.

Three producers are specified in columns $i = 2$, $i = 5$, and $i = 8$. Well 4 is a 2,000 STB/D water injector completed in Layers 13 to 15 at Column $i = 10$. Producers 1 to 3 are completed in layers 11 to 13, 2 to 14, and 1 to 5, respectively. Their target production rates are 1,000, 100, and 1,000 STB/D oil, respectively, with minimum bhp of 1,000 psia at their top perforations. Wellbore crossflow occurs in production Well 2. Layer productivity indices are calculated internally from the equation for a cross section.[35]

$$J_k = \frac{0.007084kh}{\ln(w/2\pi r_w)}\, rb - cp/d - psi, \quad \ldots\ldots\ldots\ldots\ldots\ldots (24)$$

where kh is gridblock md-ft, w is the cross section width, and r_w is equal to 0.5 ft.

Three five-year runs were made. Run 1 is the two-dimensional (2D) x-z cross section with crossflow deactivated (production is only taken from layers where gridblock pressure exceeds wellbore pressure and other layers are nonflowing). Run 2 is the same run with the wellbore crossflow calculation active. Run 3 uses a 3D 10 x 2 x 15 grid. The second slice, $j = 2$, contains only Well 2 wellbore cells with their PV's equaling actual wellbore volume. The y-direction transmissibilities connecting these wellbore cells with their neighbors in slice $j = 1$ are equal to the Well 2 layer productivity indices J_k of Runs 1 and 2. Fractional flow ($f = S$ for each phase) is used to represent the multiphase flow vertically within and out of the wellbore cells.

A comparison of results from these three runs is presented in **Table 1**, which includes original fluids in place for the three isolated regions in this problem, as well as the remaining fluids in place at the end of 5 years. Average region pressures are also presented. Note the good agreement between the 2D run with crossflow and the exact 3D run. Significant differences are observed between the no crossflow and the crossflow run.

Non-Darcy Gas Flow Example

The effects of non-Darcy flow are illustrated by means of SPE1, which has both a gas injection well and an oil producer. The maximum gas injection pressure was set equal to 7,600 psia, which is slightly higher than the value calculated vs. time for this example when non-Darcy flow is negligible. A β multiplying factor, f, of 50 for the gas injector and oil producer was used to simulate near wellbore flow effects. A comparison of the gas/oil ratio for this example with and without the effects of non-Darcy flow are presented in **Fig. 1**. The lower gas/oil ratio shown for the run with non-Darcy flow calculations is a result of both reduced gas injection and gas production.

TABLE 1—2D CROSS SECTION WITH CROSSFLOW

	Fluids in Place				
Region	Water MSTB	Oil MSTB	Gas MMscf	Average Pressure, psia	Case, Time
1	2,107	5,963	9,319	3,620	Initial conditions
2	2,034	4,950	6,882	3,646	
3	18,572	5,742	7,983	3,703	
1	2,198	4,787	3,600	1,245	2D with crossflow, 5 years
2	2,022	4,063	3,082	1,413	
3	19,205	4,525	3,218	1,533	
1	2,221	4,787	3,522	1,221	3D exact, 5 years
2	2,031	4,067	3,053	1,402	
3	19,179	4,543	3,228	1,530	
1	2,095	4,708	2,943	1,002	2D no crossflow, 5 years
2	2,033	4,862	6,761	3,497	
3	19,557	4,292	2,973	1,519	

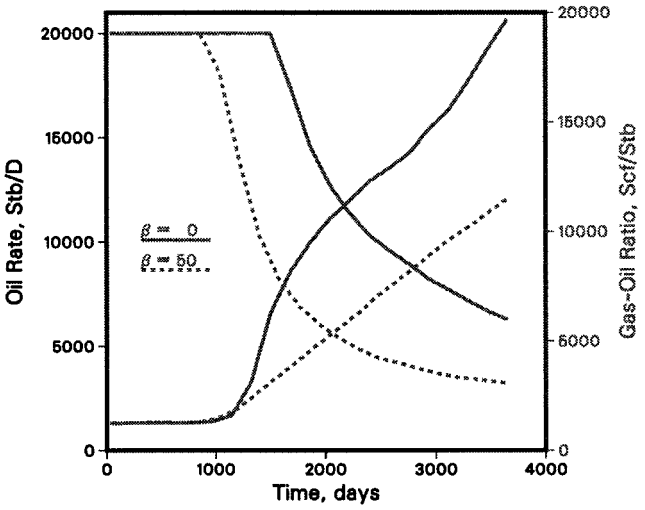

Fig. 1—SPE1 oil rate and gas/oil ratio vs. time.

The reservoir rock effect alone ($f = 1$) gives the following changes in SPE1 results at 3,650 days: cumulative gas production is reduced from 338 to 304 Bscf, and gas/oil ratio is reduced from 19,697 to 17,558 scf/STB.

SPE Comparative Solutions

Several SPE Comparative Solution examples were run during the development of the model to test the accuracy of the results and the efficiency of the formulation. Three black oil problems, SPE1, Comparison of Solutions to a 3D Black-Oil Reservoir Simulation Problem,[36] SPE2, A Three-Phase Coning Study,[37] and SPE9, An Expanded 3D Problem with a Geostatistical Distribution of Permeability,[38] were run as well as two compositional cases, SPE3, Gas Cycling of Retrograde Condensate Reservoirs,[39] and SPE5, Evaluation of Miscible Flood Simulators.[40] The number of timesteps, Newton iterations, and the CPU time required for each run are presented in **Table 2**.

The SPE1, SPE3, and SPE5 problems have square *xy* grids and are symmetrical about the diagonal $x = y$. All runs reported here used the full grids. These problems give identical results when run with the half-symmetrical element, except that CPU times are reduced by a factor of about two.

Good agreement was obtained on results from these examples and those reported previously in the literature. The oil rate and gas/oil ratio for SPE1 and the cumulative oil and gas/oil ratio for SPE5, scenario one, are presented in **Figs. 1 and 2** for illustration. Results from SPE9 are included in the comparative solution project presented by Killough.[38]

Field Examples

Two field examples are presented to demonstrate the usefulness of the model. The first example is a history match of the Ekofisk reservoir, which includes both gas and water injection. The second example is a history match of gas cycling in the Chatom reservoir.

Ekofisk

The Ekofisk field, which is located in the Norwegian sector of the North Sea, was placed on production in July 1971. Produced gas in excess of sales has been reinjected in the Crest of the field since 1975. Water injection was started in 1987 after a successful waterflood pilot was performed.[41] The waterflood was subsequently expanded,[42] and currently water injection rates average 750,000 B/D.

A history match of the field from 1971 to 1994 was run. Reservoir and production (injection) data from Phillips reservoir simulation model[43] were used as input. A 13,728-block 44 x 26 x 12 grid with all cells active was used. The Phillips model extended beta PVT data were replaced by a three-component description of Ekofisk.[28]

Field gas/oil ratio vs. time for this run is shown in **Fig. 3** along with the results from the Phillips model. Essentially identical results were obtained. The simulation was run with the IMPES formulation and took 264 timesteps, 294 iterations, and 456 seconds of CPU time applying nested factorization.

Chatom

The Smackover Reservoir of the Chatom Field, which is located in Washington County, Alabama, is a retrograde gas condensate reservoir that contains approximately 17% H_2S. Liquid content of the gas at the dewpoint pressure of 3,073 psig and reservoir temperature of 293°F is 400 bbl/MMscf. Production from the field was started in 1974, and gas injection of residue gas was initiated in 1976.

A history match of this gas cycling project from 1974 to 1994 was conducted starting with data from a previous study.[44] A

TABLE 2—SPE COMPARATIVE SOLUTION PROJECTS

Project	N_c—Grid	Formulation-Solution Algorithm	Number Timesteps	Newton Iterations	CPU Time, seconds
SPE1	2—10 × 10 × 3	Fully Implicit-NF	24	62	4.5
		IMPES-D4	254	256	7.0
SPE2	2—10 × 1 × 15	Fully Implicit-D4	15	30	2.2*
SPE3	9—9 × 9 × 4	IMPES-D4	113	114	21.5
		Fully Implicit-NF	18	28	19.8
SPE5	6—7 × 7 × 3	Scenario I			
		IMPES-D4	468	471	23.6
		FI-NF	46	172	22.3
		Scenario 2			
		IMPES-NF	654	656	19.1
		FI-NF	58	246	28.1
		Scenario 3			
		IMPES-D4	527	531	24.6
		FI-NF	47	193	26.2
SPE9	2—24 × 25 × 15	Fully Implicit-NF	33	55	62.7

* CPU time SPE2 was 0.9 sec, with 1.3 sec, for data input, initialization, and error checking. All CPU times reported in this table include similar overhead.

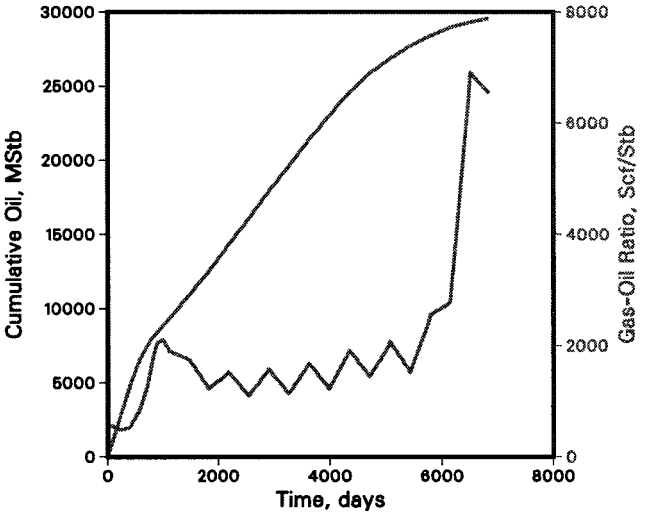

Fig. 2—SPE5 cumulative oil and gas/oil ratio vs. time.

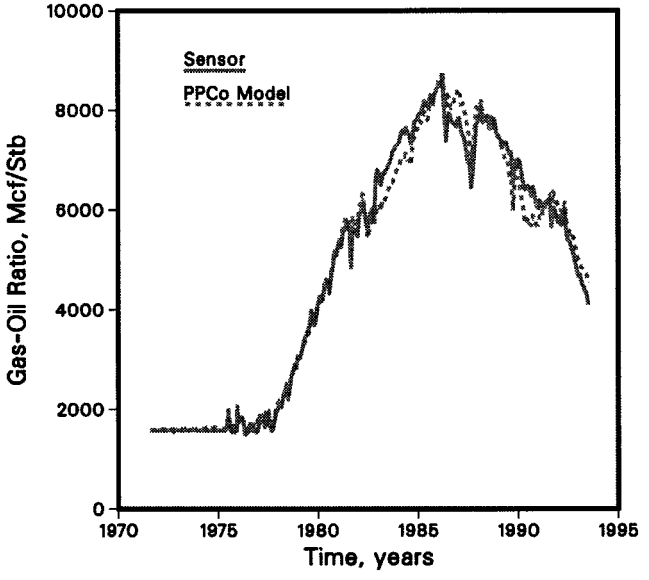

Fig. 3—Ekofisk field gas/oil ratio match.

4,056-block 26 x 26 x 6 grid with 2,214 active cells was used. The SRK EOS with six components was used to match experimental phase behavior data, which consisted of expansion and depletion experiments and swelling data. The composition of initial reservoir gas and injected gas are given in Table 1 of Ref. 44.

Results from this study are presented in **Fig. 4**, which is a comparison of calculated and actual condensate rates vs. time. This simulation took 469 timesteps, 485 iterations, and 202 CPU seconds using nested factorization.

Discussion

Several runs were made on SPE9 to investigate the level of time truncation error. Base runs applying 1- and 10-day timesteps gave essentially identical results. Next, a run with 16 timesteps and 52 iterations was made. Time truncation error in this run was apparent although not appreciably large. The last run was made with smaller maximum timestep control and took 33 timesteps and 55 Newton iterations (Table 2). The amount of time truncation error in this run is minimal.

Conclusions

1. This paper describes a general three-phase, 3D numerical simulation model. Black oil and fully compositional capabilities are included with IMPES and fully implicit formulations.

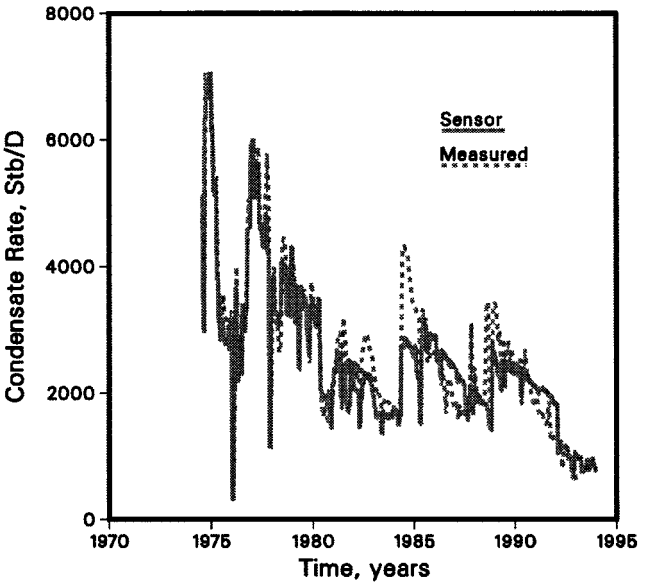

Fig. 4—Chatom condensate rate vs. time.

2. A relaxed volume concept is used in both IMPES and implicit formulations. It results in good volume balance, exact material balance, and fewer Newton iterations.

3. A new implicit treatment of well rates provides increased stability for IMPES, approximates wellbore crossflow with good efficiency and relative simplicity, and includes near-well non-Darcy gas flow effects.

4. A normalization of relative permeability and capillary pressure is presented, which allows these parameters to be calculated on a gridblock basis.

5. Example problems are presented that illustrate the utility, efficiency, and robustness of the model formulations in black oil and compositional cases.

Nomenclature

b_w = water formation volume factor, STB/b_r
c_r = rock compressibility, 1/psi
D = non-Darcy flow coefficient, d/Mcf
f = multiplier on reservoir β factor that accounts for high velocity flow through the near wellbore region
G = gas gravity, air = 1
h = layer thickness, ft
J_k = layer k productivity index, b_r-cp/d-psi
k = absolute permeability, md
k_r = relative permeability, fraction
k_{rgcw} = relative permeability to gas at connate water
k_{rwSw1} = relative permeability to water at $S_w = 1$
M = gas molecular weight
N = total number of variables, $2N_c + 4$
N_c = number of hydrocarbon components
N_w = number of active wells on target rates
p = gas phase pressure, psia
p_b = base or reference pressure
p_{sat} = saturation pressure, psia
p_w = bottomhole wellbore pressure
P = $N_c + 1$ − vector of primary variables
$\bar{P}$ = N − vector of total variables
P_c = capillary pressure, psi
P_e = N_c vector of eliminated variables
q_g = gas production rate, Mcf/D
q_i = production rate of component i, moles/D
q_w = production rate of water, moles/D
q^* = well target rate
Q = production rate, total RB/D
r_s = oil in gas phase, STB/scf
r_w = wellbore radius, ft

R_s = dissolved gas, scf/STB
s = skin factor
S = phase saturation, fraction
S_{gc} = critical gas saturation
S_{gr} = residual gas saturation
S_{org} = residual oil saturation (ROS) to gas
S_{orw} = ROS to water
S_{wc} = connate water saturation
t = time, days
Δt = timestep, days
T = transmissibility, RB-cp/d-psi
v = IMPES reduction vector
V = gridblock volume, $\Delta x \Delta y \Delta z/5.6146$, RB
x = mole fraction in liquid phase
X_1, Y_1 = mole fraction of oil in converted black oil table
y = mole fraction in gas phase
z = overall mole fraction
Z = subsea depth, ft
Z^* = reference depth for flow bottomhole pressure

Greek

α = $(1 - S_w - S_o - S_g)^l$
β = Forscheimer coefficient, 1/ft
$\bar{\delta}$ = $\bar{\delta}X = X_{n+1} - X_n$
δ = $\delta X = X_l^{+1} - X_l$
γ = gradient, psi/ft
λ = mobility, k_r/μ
μ = viscosity, cp
ρ = phase density, moles/RB
ϕ = porosity, fraction
ϕ_b = gridblock porosity at pressure p_b
τ = transmissibilities in the IMPES pressure equation

Subscripts

c = critical
g = gas
i = component number
k = layer number
l = iteration number (superscript)
n = timestep number
o = oil
w = water
wb = wellbore

Acknowledgments

We express our appreciation to Phillips Petroleum Co. for permission to publish this paper. Special thanks to Jim Sylte and Kim Juenger for helping develop the field examples presented in the paper.

References

1. Peng, D.Y. and Robinson, D.B.: "A Rigorous Method for Predicting the Critical Properties of Multicomponent Systems from an Equation of State," *AIChE J.* (1977) **23,** 137.
2. Soave, G.: "Equilibrium Constants for a Modified Redlich-Kwong Equation of State," *Chem. Eng. Sci.* (1972) **27,** 1197.
3. Jhaveri, B.S. and Youngren, G.K.: "Three-Parameter Modification of the Peng-Robinson Equation of State To Improve Volumetric Predictions," *SPERE* (August 1988) 1033.
4. Peneloux, A., Rauzy, E., and Freze, R.: "A Consistent Correction for Redlich-Kwong-Soave Volumes," *Fluid Phase Equilibria* (1982) **8**, 7.
5. Sulak, R.M., Thomas, L.K., and Boade, R.R.: "3D Reservoir Simulation of Ekofisk Compaction Drive," *JPT* (October 1991) 1272; *Trans*., AIME, **291**.
6. Hermansen, H., Thomas, L.K., Sylte, J.E., and Aasboe,B.T.: "Twenty Five Years of Ekofisk Reservoir Management," paper SPE 38927 presented at the 1997 Annual Technical Conference and Exhibition, San Antonio, Texas, 5–8 October.
7. Price, H.S. and Coats, K.H.: "Direct Methods in Reservoir Simulation," *SPEJ* (June 1974) 295–308; *Trans*, AIME, **257**.
8. Appleyard, J.R. and Cheshire, I.M., "Nested Factorization," paper SPE 12264 presented at the 1983 SPE Reservoir Simulation Symposium, San Francisco, 16–18 November.
9. Cheshire, I.M., "The Solution of Linear Equations in Implicit Simulators," *Proc*., Fourth International Forum on Reservoir Simulation, Salzburg, Austria (1992).
10. Eisenstat, S.C., Elman, H.C., and Schultz, M.H.: "Block-Preconditioned Conjugate-Gradient-Like Methods for Numerical Reservoir Simulation," *SPERE* (February 1988) 100.
11. Bansal, P.P, Harper, J.L., McDonald, A.E., Moreland, E.E., and Odeh, A.S.: "A Strongly Coupled, Fully Implicit, 3D, Three-Phase Reservoir Simulator," paper SPE 8329 presented at the 1979 SPE Annual Technical Conference and Exhibition, Las Vegas, Nevada, 23–26 September.
12. Trimble, R.H. and McDonald, A.E.,: "A Strongly Coupled, Fully Implicit, 3D, Three-Phase, Well Coning Model," *SPEJ* (August 1981) 454; *Trans*., AIME, **271**.
13. Coats, K.H.: "An Equation of State Compositional Model," *SPEJ* (October 1980) 363; *Trans*., AIME, **269**.
14. Young. L.C. and Stephenson, R.E.: "A Generalized Compositional Approach for Reservoir Simulation," *SPEJ* (October 1983) 727; *Trans*., AIME, **275**.
15. Acs, G., Doleschall, S., and Farkas, E.: "General Purpose Compositional Model," *SPEJ* (August 1985) 543; Trans., AIME, **279**.
16. Watts, J.W.: "A Compositional Formulation of the Pressure and Saturation Equations," *SPERE* (May 1986) 243; *Trans*., AIME, **281**.
17. Stone, H.L. and Garder, A.O. Jr.: "Analysis of Gas-Cap or Dissolved-Gas Drive Reservoirs," *SPEJ* (June 1961) 92; *Trans*., AIME, **222**.
18. Sheldon, J.W., Harris, C.D., and Bavly, D.: "A Method for Generalized Reservoir Behavior Simulation on Digital Computers," paper SPE 1521-G presented at the 1960 Annual SPE Fall Meeting, Denver, Colorado, 2–5 October.
19. Wattenbarger, R.A.: "Convergence of the Implicit Pressure-Explicit Saturations Method," *JPT* (November 1968) 1220.
20. Wattenbarger, R.A.: "Practical Aspects of Compositional Simulation," paper SPE 2800 presented at the 1970 SPE Second Symposium on Numerical Simulation of Reservoir Performance, Dallas, 5–6 February.
21. Abel, W., Jackson, R.F., and Wattenbarger, R.A.: "Simulation of a Partial Pressure Maintenance Gas Cycling Project with a Compositional Model, Carson Creek Field, Alberta," *JPT* (January 1970) 285.
22. Coats, K.H.: "Reservoir Simulation: A General Model Formulation and Associated Physical/Numerical Sources of Instability," *Boundary and Interior Layers - Computational and Asymptotic Methods*, J.J.H. Miller (ed.), Boole Press, Dublin, Ireland (1980) 62.
23. Fussell, L.T. and Fussell, D.D.: "An Iterative Technique for Compositional Reservoir Models," *SPEJ* (August 1979) 211.
24. Lohrenz, J., Bray, B.G., and Clark, C.R.: "Calculating Viscosity of Reservoir Fluids from their Composition," *JPT* (October 1964) 1171.
25. Reid, R.C. and Sherwood, T.K.: *The Properties of Gases and Liquids*, Third edition, McGraw-Hill Book Co. Inc., New York City (1977).
26. Holmes, J.A.: "Enhancements to the Strongly Coupled, Fully Implicit Well Model: Wellbore Crossflow Modeling and Collective Well Control," paper SPE 12259 presented at the 1983 SPE Reservoir Simulation Symposium, San Francisco, 15–18 November.
27. Modine, A.D., Coats, K.H., and M.W. Wells: "A Superposition Method for Representing Wellbore Crossflow in Reservoir Simulation," *SPERE* (August 1992) 335; *Trans*., AIME, **293**.
28. Coats, K. H.: "Engineering and Simulation," *Proc*., Fourth International Forum on Reservoir Simulation, Salzburg, Austria (1992).
29. Coats, K.H.: "Implicit Compositional Simulation of Single Porosity and Dual Porosity Reservoirs," *Proc*., First International Forum on Reservoir Simulation, Alpbach, Austria (1988).
30. Cornell, D., and Katz, D.L.: "Flow of Gases Through Consolidated Porous Media," *Industrial Engineering Chemistry* (1953) **45,** 2145.
31. Katz, D.L., *et al*.: *Handbook of Natural Gas Engineering*, McGraw-Hill Book Co., Inc., New York City (1959).
32. Firoozabadi, A. and Katz, D.L.: "An Analysis of High Velocity Gas Flow Through Porous Media," *JPT* (February 1979) 211.
33. McLeod, H.O. Jr.: "The Effect of Perforating Conditions on Well Performance," *JPT* (January 1983) 31; *Trans*., AIME, **275**.
34. Thomas, L.K., Evans, C.E., Pierson, R.G., and Scott, S.L.: "Well Performance Model," *JPT* (February 1992) 220; *Trans*., AIME, **293**.

35. Coats, K.H. and Ramesh, A.B.: "Effects of Grid Type and Difference Scheme on Pattern Steamflood Simulation Results," *JPT* (May 1986) 557.
36. Odeh, A.S.: "Comparison of Solutions to a 3D Black-Oil Reservoir Simulation Problem," *JPT* (January 1981) 13; *Trans.*, AIME, **271**.
37. Weinstein, H.G., Chappelear, J.E., and Nolen, J.S.: "Second Comparative Solution Project: A Three-Phase Coning Study," *JPT* (March 1986) 345.
38. Killough, J.H.: "Ninth SPE Comparative Solution Project: An Expanded 3D Problem with a Geostatistical Distribution of Permeability," paper SPE 29110 presented at the 1995 SPE Reservoir Simulation Symposium, San Antonio, Texas, 12–15 February.
39. Kenyon, D.E. and Behie, G.A.: "Third SPE Comparative Solution Project: Gas Cycling of Retrograde Condensate Reservoirs," *JPT* (August 1987) 981.
40. Killough, J. and Kossack, C.: "Fifth SPE Comparative Solution Project: Evaluation of Miscible Flood Simulators," paper SPE 16000 presented at the 1987 SPE Reservoir Simulation Symposium, San Antonio, Texas, 1–4 February.
41. Thomas, L.K., Dixon, T.N., Evans, C.E., and Vienot, M.E.: "Ekofisk Waterflood Pilot," *JPT* (February 1987) 221; *Trans.*, AIME, **283**.
42. Hallenbeck, L.D., Sylte, J.E., Ebbs, D.J., and Thomas, L.K.: "Implementation of the Ekofisk Waterflood," *SPEFE* (September 1991) 284; *Trans.*, AIME, **291**.
43. Thomas, L.K., Dixon, T.N. and Pierson, R.G.: "Fractured Reservoir Simulation," *SPEJ* (February 1983) 42; *Trans.*, AIME, **275**.
44. Tompkins, M.W., Ebbs, D.J., Thomas, L.K., and Dixon, T.N.: "Chatom Gas Condensate Cycling Project," SPE Advanced Technology Series (July 1993)152.
45. Land, C.S.: "Calculation of Imbibition Relative Permeability for Two- and Three-Phase Flow from Rock Properties," *SPEJ* (June 1968) 149; *Trans.*, AIME, **243**.
46. Stone, H.L.: "Estimation of Three-Phase Relative Permeability and Residual Oil Data," *J. Cdn. Pet. Tech.* (October–December 1973) 53.
47. Thomas, L.K. and Coats, K.H.: "Stone's k_{ro} Methods and Modifications," SPE paper 25289, available from Richardson, Texas, June, 1992.

Appendix

Relative Permeability

Relative permeability and capillary pressure curves are normalized by means of residual saturations, which can be entered on a gridblock basis, and normalized saturation equations for the wetting and nonwetting phases. The normalized saturations range from zero to one for mobile phase saturations. Drainage P_{cwo} and k_{rw} are normalized by means of S_w^*, where

$$S_w^* = \frac{S_w - S_{wc}}{1 - S_{wc}}. \quad \text{(A-1)}$$

Imbibition P_{cwo} and k_{row} are normalized by means of $\bar{S}_w$.

$$\bar{S}_w = \frac{S_w - S_{wc}}{1 - S_{wc} - S_{orw}}. \quad \text{(A-2)}$$

The normalized saturations for k_{rg} and k_{rog} are S_g^* and $\bar{S}_g$, respectively.

$$S_g^* = \frac{S_g - S_{gc}}{1 - S_{wc} - S_{gc}} \quad \text{(A-3)}$$

$$\bar{S}_g = \frac{S_g}{1 - S_{wc} - S_{org}}. \quad \text{(A-4)}$$

Relative permeability can be entered in tabular form or calculated from normalized saturations. If data are calculated, they are then loaded into tables. Next the tabular data are normalized for use in the model. The calculated k_r values are of Corey type, for example applying an exponent of 2 gives

$$k_{rw} = k_{rwSwl}(S_w^*)^2 \quad \text{(A-5)}$$

$$k_{row} = (1 - \bar{S}_w)^2 \quad \text{(A-6)}$$

and

$$k_{rg} = k_{rgcw}(S_g^*)^2 \quad \text{(A-7)}$$

$$k_{rog} = (1 - \bar{S}_g)^2. \quad \text{(A-8)}$$

Hysteresis in k_{rg} is calculated by means of a modification of Land's equation.[28,45] Residual gas saturation, S_{gr}, is a function of historical maximum gas saturation. Three-phase oil relative permeability is calculated by means of Stone's first method[46] with variable S_{or}[47] or optionally with Stone's second method.

SI Metric Conversion Factors

bbl × 1.589 873	E−01	= m^3
cp × 1.0*	E−03	= Pa·s
cu ft × 2.831 685	E−02	= m^3
°F (°F−32)/1.8		= °C
ft × 3.048*	E−01	= m
psi,psia × 6.894 757	E+00	= kPa
psi^{-1} × 1.450 377	E−01	= kPa^{-1}

*Conversion factors are exact.

SPEREE

Keith Coats is President of K.H. Coats and Co. Inc. in Florida. Previously, he was Assistant Professor of chemical engineering at the U. of Michigan, Associate Professor of petroleum engineering at the U. of Texas, a research associate at Esso Production Research, and Chairman of Intercomp. Coats holds MS and PhD degrees in chemical engineering and an MS degree in mathematics from the U. of Michigan. **Kent Thomas** is Manager of Engineering Sciences in the Research and Services Div. of Phillips Petroleum Co. in Bartlesville, Oklahoma. He holds a BS degree from the U. of Oklahoma and MS and PhD degrees from the U. of Michigan, all in chemical engineering. Thomas served as the Program Chairman for the 1997 SPE Symposium on Reservoir Simulation and is currently a member of the 1999 Program Committee. He was the recipient of the 1993 Reservoir Engineering Award and has served as a Distinguished Lecturer. Thomas was elected a SPE Distinguished Member in 1995. **Ray Pierson** is a senior research computing specialist at Phillips Petroleum Co. in Bartlesville. He holds a BS degree in mathematics from Southwestern Oklahoma State U.